Results in Physics 10 (2018) 107–117

Contents lists available at ScienceDirect

Results in Physics

journal homepage: www.elsevier.com/locate/rinp

Interaction between chemical species and generalized Fourier's law on 3D flow of Carreau fluid with variable thermal conductivity and heat sink/source: A numerical approach

M. Irfan[a,*], M. Khan[a], W.A. Khan[b]

[a] Department of Mathematics, Quaid-i-Azam University, Islamabad 44000, Pakistan
[b] Department of Mathematics and Statistics, Hazara University, Mansehra 21300, Pakistan

ARTICLE INFO

Keywords:
3D Carreau liquid
Variable thermal conductivity
Cattaneo–Christov heat conduction relation
Heat sink/source
Homogeneous-heterogeneous reactions

ABSTRACT

This paper deals with three-dimensional (3D) flow of a Carreau fluid by utilizing the impact of heterogeneous-homogeneous reactions towards the bidirectional stretched surface. The heat transfer mechanism is carried out in apparition of improved heat conduction relation. This occurrence is documented upon the notion of generalized Fourier's law that contributes by the thermal relaxation. Additionally, temperature dependent thermal conductivity and heat sink/source are accounted. On utilization of a suitable conversions a system of nonlinear ordinary differential equation (ODEs) is attained and then inferred numerically via bvp4c approach. The delineations of velocities, temperature and concentration fields corresponding to the numerous somatic parameters are scrutinized explicitly. The impact of local Weissenberg number We_1 on $f'(\eta)$ and We_2 on $g'(\eta)$ are same for (n = 0.5 and 1.5). Furthermore, our inspection spectacles that the concentration of the Carreau liquid decays as the heterogeneous-homogeneous reaction (k_2,k_1) parameters boost up. It is also remarkable that for shear thinning ($n < 1$) fluid the influence of local Weissenberg numbers (We_1,We_2) are absolutely contradictory as associated with the case of shear thickening ($n > 1$) fluid. For authentication of numerical outcomes a comparison table is prepared via benchmarking with formerly itemized limiting cases and we pledge a marvelous communication with these results. Additionally, graphically assessment is presented between numerically (bvp4c) and analytically (HAM) techniques with tremendous settlement.

Introduction

Recently, combining energetic liquids with heat transfer has been unique, worthwhile subject owing to its countless methodological and systematic solicitations. With the intention to attain the superiority of the product it is documented that the amount of cooling is noteworthy. For instance, cut-glass foodstuffs, gemstone developing, polymer dispensation, crust of cords, purify- caution of liquefied metals and canvas material, etc. The heat transport mechanism transpires when the temperature of the body or different quantities of body is changed. This procedure has enormous solicitations in power cohort, heat conduction in nerves, nuclear synthesis and countless industrial arenas. The features of heat transfer around 200 eons former, was first wished-for Fourier [1], which is the best heat conduction model to contribute an information to understand the mechanism of heated conversation in numerous circumstances. But, Fourier's law is insufficient owing to the circumstance of the initial disruption that can be controlled straightaway all over the system. Afterwards, Cattaneo [2] established an amendment of Fourier's law for heat transfer in an obstinate form. By insertion of thermal relaxation time aspect to present the thermal inertia, which is recognized as Maxwell–Cattaneo law he reformed the Fourier's law. By observance this in a vision, by interchanging time derivative with Oldroyd upper convected derivative this notion is additionally improved by Christov [3] and entitled it as Cattaneo–Christov heat flux model. For the scrutiny of convective heat transport this model is precise worthwhile. In outlook of these heat transfer properties, numerous investigators formerly have scrutinized diverse rheological problems with numerous method and physical facets (Refs. [4–9]). These research determined that intensifying the thermal relaxation time heightens the heat transfer amount by bearing in mind the theory of Cattaneo–Christov heat flux. For instance, Mustafa et al. [10] scrutinized the theory of upgraded heat flux relation on Maxwell liquids with the impact of variable thermal conductivity in rotating frame analytically. They point out that owing to the insertion of elastic properties the hydrodynamic boundary layer turn out to be thinner. Furthermore, Ali and Sandeep [11] reported numerically, the impact of the improved

* Corresponding author.
E-mail address: mirfan@math.qau.edu.pk (M. Irfan).

https://doi.org/10.1016/j.rinp.2018.04.036
Received 7 December 2017; Received in revised form 13 March 2018; Accepted 14 April 2018
Available online 24 April 2018
2211-3797/ © 2018 Published by Elsevier B.V. This is an open access article under the CC BY-NC-ND license (http://creativecommons.org/licenses/BY-NC-ND/4.0/).

Nomenclature

u,v,w	velocity components
x,y,z	space coordinates
ν	kinematic viscosity
Γ	material rate constant
n	power law index
$(\rho c)_f$	heat capacity of fluid
T	temperature of fluid
$K(T)$	variable thermal conductivity
k_∞	thermal conductivity far away from stretched surface
T_∞	ambient fluid temperature
Q_0	heat sink/source coefficient
λ	thermal relaxation time coefficient
G, H	chemical species
g, h	concentration of chemical species
k_c, k_s	rate constants
D_G, D_H	diffusion species coefficients
a, b	positive constants
$U_w(x)$, $V_w(x)$	stretching velocities
p	pressure
(μ_0, μ_∞)	zero and the infinity shear-rate viscosities
$\dot{\gamma}$	shear rate
$\mathbf{A}_1$	first Rivlin-Erickson tensor
S^*	Cauchy stress tensor
η	dimensionless variable
We_1, We_2	local Weissenberg numbers
β	thermal relaxation time parameter
Pr	Prandtl number
	heat source parameter
$\delta < 0$	heat sink parameter
Sc	Schmidt number
k_1	homogeneous reaction parameter
k_2	heterogeneous reaction parameter
α	ratio of stretching rates parameter
ϵ	thermal conductivity parameter
λ_1	the ratio of diffusion coefficient
τ_{xz}, τ_{yz}	surface shear stresses along x and y directions
C_{fx}, C_{fy}	skin friction coefficients
Re_x	local Reynolds number
f, g	dimensionless velocities
θ	dimensionless temperature
l	dimensionless concentration

heat flux theory for radiative flow of magnetite Casson-ferrofluid. These upshots specified that thermal relaxation parameter efficiently augments the local Nusselt number and the heat transfer enactment is extraordinary in the case of flow towards a wedge when related to flow towards plate/cone. Dogonchi and Ganji [12] investigated the combined features of thermal radiation and MHD on nanofluid between parallel plates by utilizing the theory of Cattaneo–Christov heat flux. They stated that the Nusselt number has revers impact for thermal relaxation and heat source parameters.

In recent times, hydrogen-fueled and hydro-carbon homogeneous/heterogeneous micro reactors have been the attention of forceful exertions for an impartially wide-ranging assortment of moveable constructions of energy with established energy compactness considerably sophisticated than those of the advanced Li-ion batteries. The solicitations of micro reactors assortment from catalytic micro reactors recycled for the steam revolutionizing of hydrocarbon fuel in little and high-temperature energy chambers and to micro-scale heat apparatuses, in which a catalytic micro combustor is recycled for straight chemical-to-thermal energy exchange. In furthermost cases, reinforced moral metallic catalysts are engaged owing to their extraordinary biochemical bustle and constancy for the catalytic restructuring and oxidation of hydrocarbons and hydrogen.

Studies on the subject of chemical reaction have attained uninterrupted thoughtfulness from the modern technologists and engineers. The intrinsic way of a chemical reaction happens if two or more reactants yield a product. These chemical reactions are noteworthy in numerous processes like atmospheric flows, hydrometallurgical diligence, mutilation of crops, fabrication of polymer and porcelains, fog materialization and dispersal. At diverse amounts the relation among these reactions together with consumption and fabrication of reactant kinds inside liquid and on catalytic surface is reasonably convoluted. Apart from in the manifestation of a catalyst numerous reactions have the aptitude to transfer gradually or not at all. The viscous fluid flow with the impact of features of heterogeneous/homogeneous processes was scrutinized by Merkin [13] who wished-for an isothermal relation. Moreover, by seeing both kinds of the equal diffusivities, Chaudhry and Merkin [14] discussed the properties of heterogeneous/homogeneous reactions in a viscous liquid. In diverse facets countless studies for flow with heterogenous/homogeneous reactions are pointed out via (Refs. [15–19]). For instance, Numerically, reported the impact of chemical reactions subject to nonlinear radiative flow and variable thicked surface was examined by Khan et al. [20]. Xu [21] explored the liquid flow in the stagnation area with the influence of heterogeneous-homogeneous reaction. He reported multiple solutions numerically via hysteresis bifurcation approach and showed that Prandtl number and homogeneous reaction parameter was not the reasons to produce multiple solutions. By utilizing the facets of homogeneous-heterogeneous reactions on 3D radiative flow of magneto nanoliquid was analyzed by Hayat et al. [22]. They showed that homogeneous and heterogeneous reaction parameters have conflicted trend on concentration field. Khan et al. [23] investigated numerically the aspects of chemical species on unsteady 3D magnetite Carreau liquid. The properties of shear thinning/thickening was also reported and these outcomes specified that the concentration of Carreau liquid decayed for homogeneous reaction and unsteadiness parameters.

Till date, as a consequence of enormous industrial applications the notion of non-Newtonian liquids have dragged much thoughtfulness when equated to Newtonian liquids. Moreover, plenty of experimental and notional studies have been executed to scrutinize the mechanism of non-Newtonian transport owing to their extensive applications in numerous genetic and developed progressions, materials and motorized engineering. Numerous materials, for instance biomedical flows, splashes, bio-fluids in genetic material and polymers are identified as non-Newtonian liquids. In spite of all such concentrations, countless investigators are quiet engaged to scrutinize the analysis of non-Newtonian liquids under diverse prospective. Thus, countless communications for non-Newtonian constituents have been wished-for (Refs. [24–32]). Up till now well-designed Carreau fluid [33] is a constitutive model which was formerly wished-for to pretend the properties of shear thinning/thickening liquids of non-Newtonian liquids. For instance, Sulochana et al. [34] numerically via RK with shooting procedure examined the impact of stagnation point on Carreau nanofluid. They described that the magnetic parameter has tendency to control the flow field. Recently, Khan et al. [35] anticipated a new model for 3D flow of Carreau fluid with nonlinear thermal radiation. Later on, Khan et al. [36,37] and Irfan et al. [38] scrutinized by extending the notion of 3D flow of Carreau fluid by taking diverse properties. In these scrutiny they described that thermal Biot number, Brownian, thermophrosis and thermal radiation parameters enhanced the temperature field respectively. A revised relation of nanoparticles in radiative magnetite Carreau fluid was presented by Waqas et al. [39].

Keeping the above literatures in notice, the notable thoughtfulness

here is to explore the features of chemical reactions and improved heat conduction theory on 3D flow of Carreau fluid. The stimulus of temperature dependent thermal conductivity [40–42] with heat sink/source [43–48] are also presented. Compatible conversions change the PDEs into ODEs which is then elucidated numerically via bvp4c approach. Upshots are deduced for the influential variables which appear in this analysis. It is wished that current scrutiny will be responsible for a platform for advance investigation on this subject matter in forthcoming.

Physical model and mathematical formulation

Rheological models

The present analysis emphases on time independent generalized Newtonian liquid that follows the rheological structures of the Carreau fluid model. The Cauchy stress tensor for the Carreau fluid model is specified by the following expression

$$\tau = -p\mathbf{I} + \mu(\dot{\gamma})\mathbf{A}_1, \tag{1}$$

with

$$\mu(\dot{\gamma}) = \mu_\infty + (\mu_0 - \mu_\infty)[1 + (\Gamma\dot{\gamma})^2]^{\frac{n-1}{2}}, \tag{2}$$

here, p is the pressure, $\mathbf{I}$ the identity tensor, (μ_0, μ_∞) the zero and the infinity shear-rate viscosities, respectively, n the power law exponent, Γ the material time constant, $\mathbf{A}_1 = \nabla\mathbf{V} + (\nabla\mathbf{V})^T$ the first Rivlin-Erickson tensor and the shear rate is defined by

$$\dot{\gamma} = \sqrt{\frac{1}{2}tr(\mathbf{A}_1^2)}. \tag{3}$$

In view of the most useful circumstances, $\mu_0 \gg \mu_\infty$ and μ_∞ is assumed to be zero. Hence, in consideration of Eq. (2), Eq. (1) reduces to the following form

$$\tau = -p\mathbf{I} + \mu_0[1 + (\Gamma\dot{\gamma})^2]^{\frac{n-1}{2}}\mathbf{A}_1. \tag{4}$$

Note that the range of power law index $0 < n < 1$ terms the shear thinning or pseudoplastic liquid and $n > 1$ terms the shear thickening or dilatant liquid in Carreau fluid model.

Governing equations

The constitutive flow equation for 3D steady, incompressible Carreau fluid in vectorial form can be written as follows:

$$\text{div}\,\mathbf{V} = 0, \tag{5}$$

$$\rho_f(\mathbf{V}\cdot\nabla)\mathbf{V} = \nabla\cdot\mathbf{S}^*, \tag{6}$$

where $\mathbf{V}$ is the velocity vector, ρ_f the liquid density, $\mathbf{S}^*$ the Cauchy stress tensor.

For steady 3D flow, we seeks the velocity and Cauchy stress tensor of the form

$$\mathbf{V} = [u(x,y,z), v(x,y,z), w(x,y,z)], \quad \mathbf{S}^* = \mathbf{S}(x,y,z). \tag{7}$$

Now substituting Eq. (7) in Eqs. (5)–(6), having in mind Eqs. (3) and (4), a lengthy but straight forward calculations, yields the following boundary layer equations for the steady 3D flow of Carreau fluid.

$$\frac{\partial u}{\partial x} + \frac{\partial v}{\partial y} + \frac{\partial w}{\partial z} = 0, \tag{8}$$

$$u\frac{\partial u}{\partial x} + v\frac{\partial u}{\partial y} + w\frac{\partial u}{\partial z} = -\frac{1}{\rho_f}\frac{\partial p}{\partial x} + \nu\frac{\partial^2 u}{\partial z^2}\left[1 + \Gamma^2\left(\frac{\partial u}{\partial z}\right)^2\right]^{\frac{n-1}{2}} + \nu\left(\frac{\partial u}{\partial z}\right)\frac{\partial}{\partial z}\left[1 + \Gamma^2\left(\frac{\partial u}{\partial z}\right)^2\right]^{\frac{n-1}{2}}, \tag{9}$$

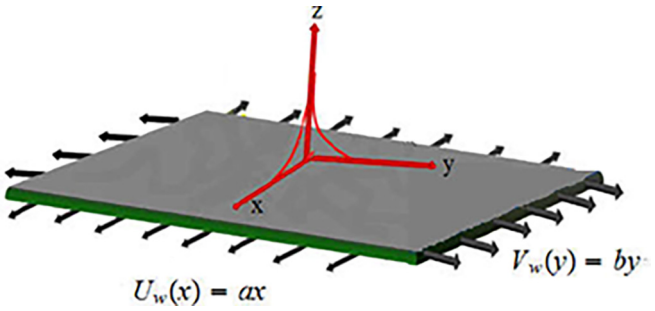

Fig. 1. Flow configuration.

$$u\frac{\partial v}{\partial x} + v\frac{\partial v}{\partial y} + w\frac{\partial v}{\partial z} = -\frac{1}{\rho_f}\frac{\partial p}{\partial y} + \nu\frac{\partial^2 v}{\partial z^2}\left[1 + \Gamma^2\left(\frac{\partial v}{\partial z}\right)^2\right]^{\frac{n-1}{2}} + \nu\left(\frac{\partial v}{\partial z}\right)\frac{\partial}{\partial z}\left[1 + \Gamma^2\left(\frac{\partial v}{\partial z}\right)^2\right]^{\frac{n-1}{2}}, \tag{10}$$

Problem formulations

Let we consider the steady 3D flow of a Carreau fluid influenced by a bidirectional stretched surface. The sheet is stretched with velocities $(u,v) = (ax,by)$ respectively, in which $a,b > 0$ are positive constants and flow occupies the domain $z > 0$ (as portrayed in Fig. 1). The heat transfer mechanism is occupied in the manifestation heat sink/source, variable thermal conductivity and an Cattaneo–Christov heat conduction relation. Moreover, the impact of heterogeneous-homogeneous chemical reactions are taken into account. Homogeneous reactions for cubic autocatalysis can be termed as:

$$G + 2H \to 3H, \quad \text{rate} = k_c g h^2, \tag{11}$$

whereas, the isothermal reaction of the first-order on the catalyst surface is of the form

$$G \to H, \quad \text{rate} = k_s g, \tag{12}$$

in which (G,H) are the chemical species which have the concentration (g,h) and rate constants (k_c,k_s), respectively. Furthermore, it is assumed that both the reactions are isothermal and distant from the sheet at the ambient fluid, for reactant G there is a uniform concentration g_0, while there is no autocatalyst H.

The Carreau fluid flow problem with boundary conditions [20,23,35] under these attentions are written as:

$$\frac{\partial u}{\partial x} + \frac{\partial v}{\partial y} + \frac{\partial w}{\partial z} = 0, \tag{13}$$

$$u\frac{\partial u}{\partial x} + v\frac{\partial u}{\partial y} + w\frac{\partial u}{\partial z} = \nu\frac{\partial^2 u}{\partial z^2}\left[1 + \Gamma^2\left(\frac{\partial u}{\partial z}\right)^2\right]^{\frac{n-1}{2}} + \nu(n-1)\Gamma^2\left(\frac{\partial u}{\partial z}\right)^2\frac{\partial^2 u}{\partial z^2}\left[1 + \Gamma^2\left(\frac{\partial u}{\partial z}\right)^2\right]^{\frac{n-3}{2}}, \tag{14}$$

$$u\frac{\partial v}{\partial x} + v\frac{\partial v}{\partial y} + w\frac{\partial v}{\partial z} = \nu\frac{\partial^2 v}{\partial z^2}\left[1 + \Gamma^2\left(\frac{\partial v}{\partial z}\right)^2\right]^{\frac{n-1}{2}} + \nu(n-1)\Gamma^2\left(\frac{\partial v}{\partial z}\right)^2\frac{\partial^2 v}{\partial z^2}\left[1 + \Gamma^2\left(\frac{\partial v}{\partial z}\right)^2\right]^{\frac{n-3}{2}}, \tag{15}$$

$$u\frac{\partial T}{\partial x}+v\frac{\partial T}{\partial y}+w\frac{\partial T}{\partial z}=\frac{1}{(\rho c)_f}\frac{\partial}{\partial z}\left(K(T)\frac{\partial T}{\partial z}\right)+\lambda\begin{bmatrix}u^2\frac{\partial^2 T}{\partial x^2}+v^2\frac{\partial^2 T}{\partial y^2}+w^2\frac{\partial^2 T}{\partial z^2}+2uv\frac{\partial^2 T}{\partial x\partial y}\\+2vw\frac{\partial^2 T}{\partial y\partial z}+2uw\frac{\partial^2 T}{\partial x\partial z}+\left(u\frac{\partial u}{\partial x}+v\frac{\partial u}{\partial y}+w\frac{\partial u}{\partial z}\right)\frac{\partial T}{\partial x}\\+\left(u\frac{\partial v}{\partial x}+v\frac{\partial v}{\partial y}+w\frac{\partial v}{\partial z}\right)\frac{\partial T}{\partial y}+\left(u\frac{\partial w}{\partial x}+v\frac{\partial w}{\partial y}+w\frac{\partial w}{\partial z}\right)\frac{\partial T}{\partial z}\end{bmatrix}+\frac{\lambda Q_0}{(\rho c)_f}\left(u\frac{\partial T}{\partial x}+v\frac{\partial T}{\partial y}+w\frac{\partial T}{\partial z}\right)+\frac{Q_0(T-T_\infty)}{(\rho c)_f}, \tag{16}$$

$$u\frac{\partial g}{\partial x}+v\frac{\partial g}{\partial y}+w\frac{\partial g}{\partial z}=D_G\frac{\partial^2 g}{\partial z^2}-k_c g h^2, \tag{17}$$

$$u\frac{\partial h}{\partial x}+v\frac{\partial h}{\partial y}+w\frac{\partial h}{\partial z}=D_H\frac{\partial^2 h}{\partial z^2}+k_c g h^2, \tag{18}$$

$$u=U_w(x)=ax,\quad v=V_w(y)=by,\quad w=0,$$
$$T=T_w,\quad D_G\frac{\partial g}{\partial z}=k_s g,\quad D_H\frac{\partial h}{\partial z}=-k_s g\quad \text{at}\quad z=0, \tag{19}$$

$$u\to 0,\quad v\to 0,\quad T\to T_\infty,\quad g\to g_0,\quad h\to 0\quad \text{as}\quad z\to\infty, \tag{20}$$

where (u,v,w) represent the velocity components along x-, y- and z-direction, respectively, Γ the material rate constant, n the power law index, ν the kinematic viscosity, T the liquid temperature, λ the thermal relaxation time, Q_0 the heat sink/source coefficient and (D_G,D_H) the diffusion species coefficients of G and H, respectively and $K(T)$ the temperature dependent thermal conductivity of Carreau liquid which is define as

$$K(T)=k_\infty\left(1+\epsilon\left(\frac{T-T_\infty}{T_w-T_\infty}\right)\right), \tag{21}$$

where (k_∞,ϵ) respectively, the ambient liquid thermal conductivity and small scalar parameter.

Appropriate conversions

$$u=axf'(\eta),\quad v=byg'(\eta),\quad w=-\sqrt{a\nu}\,[f(\eta)+g(\eta)],$$
$$\theta(\eta)=\frac{T-T_\infty}{T_w-T_\infty},\quad g=g_0 l(\eta),\quad h=h_0 m(\eta),\quad \eta=z\sqrt{\frac{a}{\nu}}. \tag{22}$$

Overhead conversions yield the equation of continuity satisfy identically and Eqs. (14) to (20) into following ODEs of Carreau fluid

$$f'''[1+We_1^2 f''^2]^{\frac{n-3}{2}}[1+nWe_1^2 f''^2]-f'^2+f''(f+g)=0, \tag{23}$$

$$g'''[1+We_2^2 g''^2]^{\frac{n-3}{2}}[1+nWe_2^2 g''^2]-g'^2+g''(f+g)=0, \tag{24}$$

$$(1+\varepsilon\theta)\theta''+\varepsilon\theta'^2+\Pr(f+g)\theta'-\Pr\beta[(f+g)(f'+g')\theta'+(f+g)^2\theta''-\delta f\theta']+\Pr\delta\theta=0, \tag{25}$$

$$\frac{1}{Sc}l''+(f+g)l'-k_1 l m^2=0, \tag{26}$$

$$\frac{\lambda_1}{Sc}m''+(f+g)m'+k_1 l m^2=0, \tag{27}$$

$$f(0)=0,\quad g(0)=0,\quad f'(0)=1,\quad g'(0)=\alpha,\quad \theta(0)=1, \tag{28}$$

$$l'(0)=k_2 l(0),\quad \lambda_1 m'(0)=-k_2 l(0), \tag{29}$$

$$f'\to 0,\quad g'\to 0,\quad \theta\to 0,\quad \text{as}\quad \eta\to\infty \tag{30}$$

$$l\to 1,\quad m\to 0\quad \text{as}\quad \eta\to\infty. \tag{31}$$

Here, $(We_1,We_2)=\left(\sqrt{\frac{\Gamma^2 aU_w^2}{\nu}},\sqrt{\frac{\Gamma^2 aV_w^2}{\nu}}\right)$ are the local Weissenberg numbers, $\beta(=\lambda a)$ the thermal relaxation time parameter, $\delta\left(=\frac{Q_0}{a(\rho c)_f}\right)$ the heat sink/source parameter, $\Pr\left(=\frac{\nu}{\alpha_1}\right)$ the Prandtl number, $\alpha\left(=\frac{b}{a}\right)$ the ratio of stretching rates parameter, $\lambda_1\left(=\frac{D_H}{D_G}\right)$ the ratio of diffusion coefficient, $Sc\left(=\frac{\nu}{D_G}\right)$ the Schmidt number, and (k_2,k_1) the measures the strength of heterogenous-homogeneous processes.

In physical circumstances, the diffusion coefficients D_G and D_H are taken to be equivalent i.e. $\lambda_1=1$, which will provide us

$$l(\eta)+m(\eta)=1. \tag{32}$$

Now subsequently, Eqs. (26) and (27) with boundary conditions (29) and (31) yields

$$\frac{1}{Sc}l''+(f+g)l'-k_1(1-l)^2 l=0, \tag{33}$$

$$l'(0)=k_2 l(0),\quad l\to 1\quad \text{as}\quad \eta\to\infty. \tag{34}$$

Physical quantities:

The skin friction coefficients

An crucial properties of flow are the local skin friction coefficients (C_{fx},C_{fy}) which are defined as

$$C_{fx}=\frac{\tau_{xz}}{\frac{1}{2}\rho_f U_w^2}\quad\text{and}\quad C_{fy}=\frac{\tau_{yz}}{\frac{1}{2}\rho_f U_w^2}, \tag{35}$$

in the dimensionless forms

$$\frac{1}{2}C_{fx}\,\mathrm{Re}_x^{\frac{1}{2}}=f''(0)[1+We_1^2 f''^2(0)]^{\frac{n-1}{2}}, \tag{36}$$

$$\frac{1}{2}\left(\frac{U_w}{V_w}\right)C_{fy}\,\mathrm{Re}_x^{\frac{1}{2}}=g''(0)[1+We_2^2 g''^2(0)]^{\frac{n-1}{2}}, \tag{37}$$

in which $\mathrm{Re}_x=ax^2/\nu$ is local Reynolds number.

Implementation of the method

Numerical scheme

In this breakdown, bvp4c method is betrothed to discretize the flow, energy and concentration equations for the well-planned problem. To attain this objective, we revise the Eqs. (23)–(25), (28), (30), (33) and (34) into first order differential structures are as follows:

$$f=y_1,\quad f'=y_2,\quad f''=y_3,\quad f'''=y_3', \tag{38}$$

$$g=y_4,\quad g'=y_5,\quad g''=y_6,\quad g'''=y_6', \tag{39}$$

$$\theta=y_7,\quad \theta'=y_8,\quad \theta''=y_8', \tag{40}$$

$$\phi=y_9,\quad \phi'=y_{10},\quad \phi''=y_{10}', \tag{41}$$

$$y_3'=\frac{-(y_1+y_4)y_3+y_2^2}{\Lambda_1},\quad \Lambda_1=(1+nWe_1^2 y_3^2)(1+We_1^2 y_3^2)^{\frac{n-3}{2}}, \tag{42}$$

$$y_6'=\frac{-(y_1+y_4)y_6+y_5^2}{\Lambda_2},\quad \Lambda_2=(1+nWe_2^2 y_6^2)(1+We_2^2 y_6^2)^{\frac{n-3}{2}}, \tag{43}$$

$$y_8'=\frac{-\Pr(y_1+y_4)y_8-\epsilon y_8^2-\Pr\beta\delta(y_1+y_4)y_8-\Pr\delta y_7+\Pr\beta(y_1+y_4)(y_2+y_5)y_8}{\Lambda_3} \tag{44}$$

$$\Lambda_3=(1+\epsilon y_7)-\Pr\beta(y_1+y_4)^2, \tag{45}$$

$$y_{10}'=-Sc(y_1+y_4)+Sck_1(1-y_9)y_9, \tag{46}$$

$$y_1(0)=0,\quad y_2(0)=1,\quad y_2(\infty)=0, \tag{47}$$

$$y_4(0)=0,\quad y_5(0)=\alpha,\quad y_5(\infty)=0, \tag{48}$$

$$y_7(0) = 0, \quad y_7(\infty) = 0, \tag{49}$$

$$y_{10}(0) = k_2 y_9(0) = 0, \quad y_9(\infty) = 1. \tag{50}$$

Analysis of results

To disclose the enactment of diverse parameters of present problem this section is systematized. The graphs for velocities, temperature and concentration fields are prepared. Additionally, graphical comparison along with assessment tables are also structured and discussed. Moreover, the significance of numerous somatic variables corresponding to, local Weissenberg number $We_1(0 \leqslant We_1 \leqslant 3)$, local Weissenberg number $We_2(0 \leqslant We_2 \leqslant 9)$, thermal relaxation parameter $\beta(0 \leqslant \beta \leqslant 0.3)$, thermal conductivity parameter $\epsilon(0.1 \leqslant \epsilon \leqslant 0.7)$, ratio of stretching rates parameter $\alpha(0 \leqslant \alpha \leqslant 0.6)$, Schmidt number $Sc(1 \leqslant Sc \leqslant 2)$, homogeneous parameter $k_1(0.1 \leqslant k_1 \leqslant 1.1)$ and heterogenous parameter $k_2(0.1 \leqslant k_2 \leqslant 0.7)$ on velocity, temperature and concentration fields are studies on physical point of assessment.

Behavior of We_1 on $f'(\eta)$ and $\theta(\eta)$

The feature of essential physical consideration of Carreau fluid, namely the local Weissenberg number We_1 on velocity component $f'(\eta)$ and temperature of Carreau liquid $\theta(\eta)$ for both shear thinning/thickening fluids are plotted in Fig. 2(a,b,c,d). On the basis of these sketches we noted that the We_1 decline the velocity field for shear thinning liquid, however it enhances for shear thickening liquid. Instead, totally conflicting behavior is being observed for temperature of Carreau liquid. Physically, the relaxation time of Carreau liquid particles increase when we enhance We_1. Therefore, the struggle is encountered by these particles which decay the velocity field, whereas conflicting trend is being established for shear thickening circumstance on velocity field. Moreover, the behavior of We_1 on temperature is quite reverse when compared with velocity for both instances.

Behavior of We_2 on $g'(\eta)$ and $\theta(\eta)$

Fig. 3(a,b,c,d) are interested to envision the impact of the local Weissenberg number We_2 on velocity component $g'(\eta)$ and temperature field $\theta(\eta)$ for higher values of We_2 for ($n = 0.5$ and $n = 1.5$). These plots display that augmenting values of We_2 reduce the velocity field for ($n = 0.5$) and temperature field for ($n = 1.5$), although the behavior is noted quite opposite for the velocity component ($n > 1$) and for temperature field ($n < 1$). Physically, intensifying values of the We_2 causes intensification in the liquid viscosity. Hence, the flow becomes struggle more which heighten the liquid temperature for shear thinning and decline for shear thickening liquid as disclosed in Fig. 3(c,d).

Behavior of β and ϵ on $\theta(\eta)$

To picture the properties of thermal relaxation parameter β and thermal conductivity parameter ϵ for both instances ($n < 1$ and $n > 1$) on Carreau liquid temperature field $\theta(\eta)$ Figs. 4(a,b) and 5(a,b) are exposed. Fig. 4(a,b) spectacles retreating performance for augmenting values of β for both cases. When the values of β enhance, then the liquid material necessities additional time for heat transport to adjacent elements. Therefore, the temperature gradient of Carreau liquid is high which decay the temperature field. Instead of this, it is also noticed that

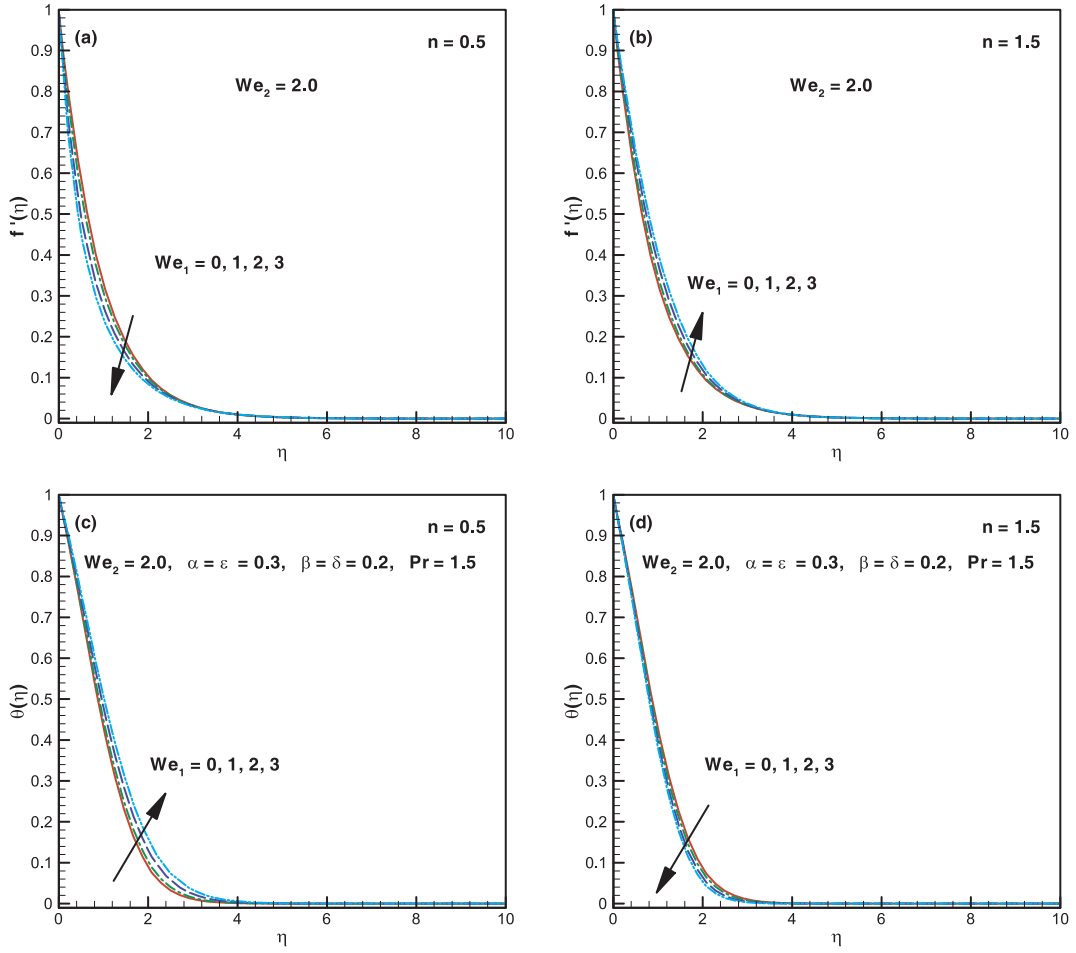

Fig. 2. (a)–(d): Impact of We_1 on $f'(\eta)$ and $\theta(\eta)$.

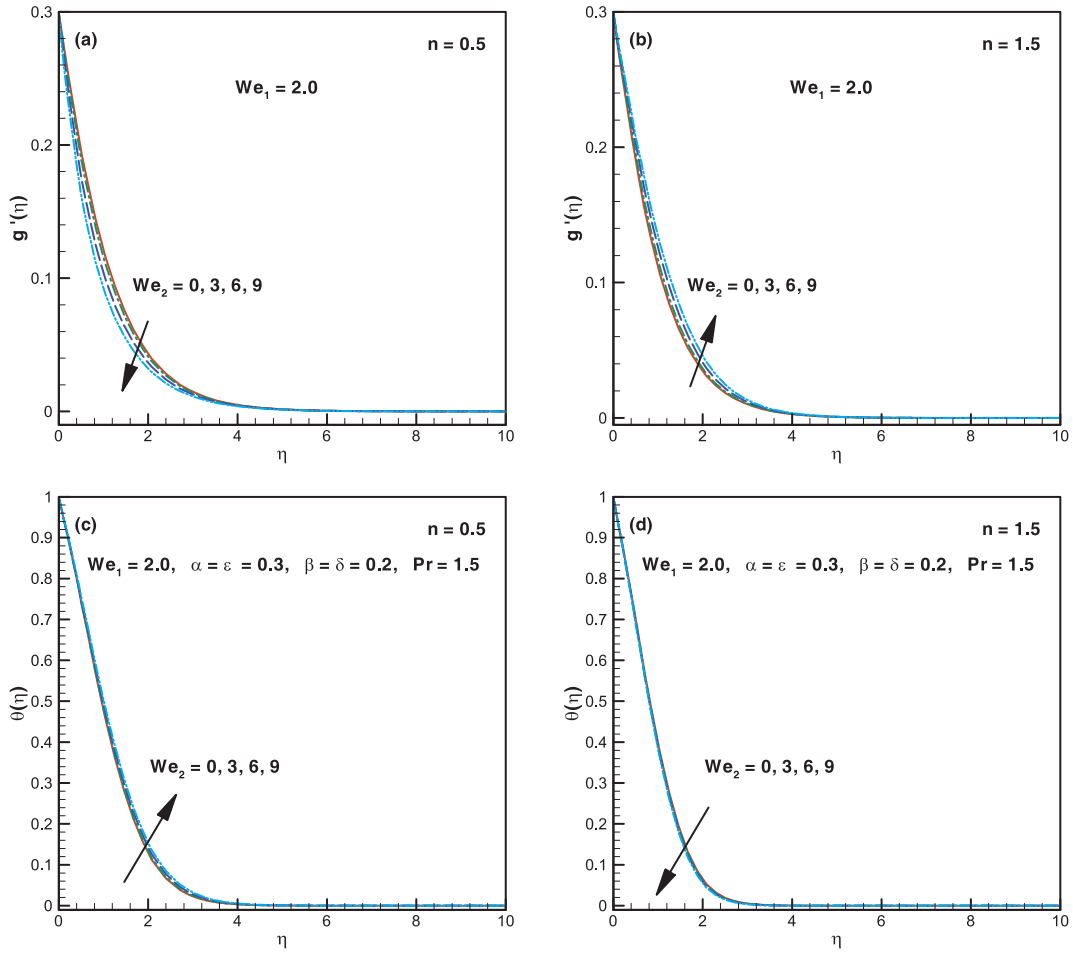

Fig. 3. (a)–(d): Impact of We_2 on $g'(\eta)$ and $\theta(\eta)$.

in both instances ($n < 1$ and $n > 1$) the thermal conductivity parameter ϵ is the enhancing function of the Carreau liquid temperature field. This happens when ϵ increase then considerable heat transfers from the sheet to the material which enhance the temperature of Carreau liquid.

Behavior of We_1 and We_2 on $l(\eta)$

The concentration field for essential parameters of Carraeu fluid the local Weissenberg numbers We_1 and We_2 for shear thinning/thickening liquids are designed in Figs. 6(a,b) and 7(a,b). Increasing values of We_1 and We_2 for ($n = 0.5$) diminish the concentration field while for ($n = 1.5$) these parameters are boosting function of concentration of Carreau liquid. Hence, at the end, we can declare that the behavior of We_1 and We_2 for shear thinning liquid is quite conflicting to shear thickening liquid on the concentration of Carreau liquid.

Behavior of α and Sc on $l(\eta)$

The plots of increasing the value of the ratio of stretching rates parameter α and Schmidt number Sc for ($n = 0.5$ and $n = 1.5$) on the

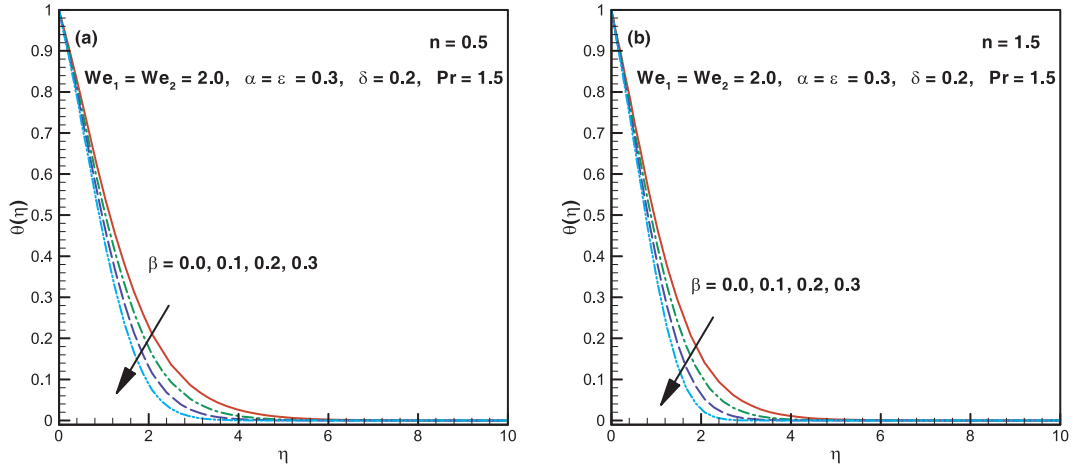

Fig. 4. (a,b): Impact of β on $\theta(\eta)$.

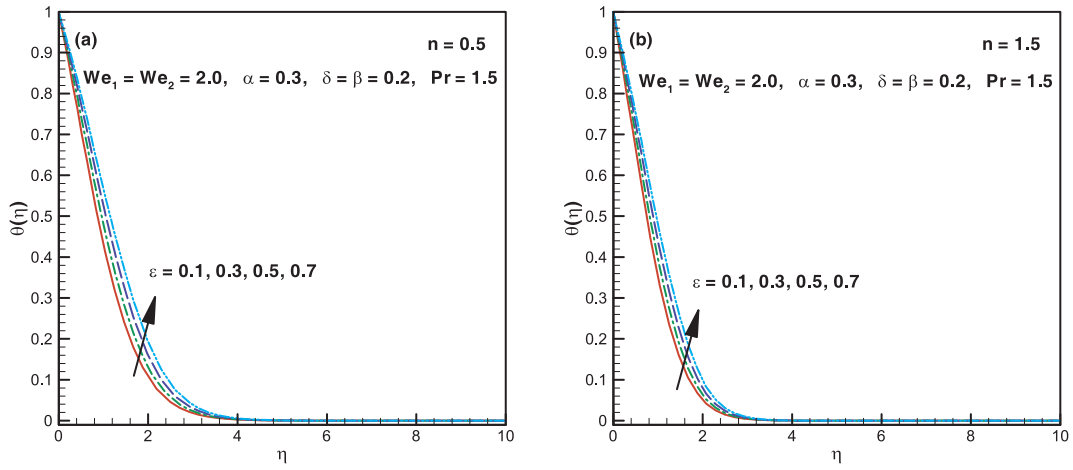

Fig. 5. (a,b): Impact of ϵ on $\theta(\eta)$.

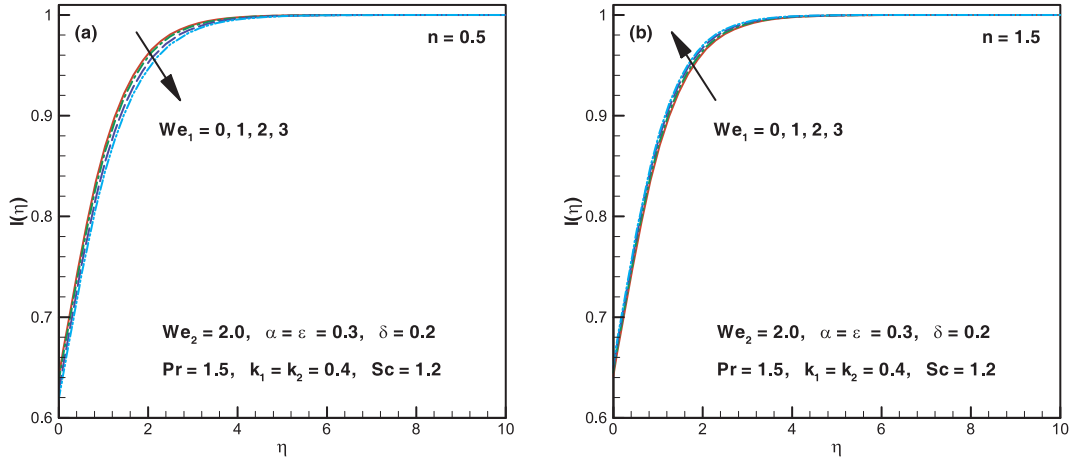

Fig. 6. (a,b): Impact of We_1 on $l(\eta)$.

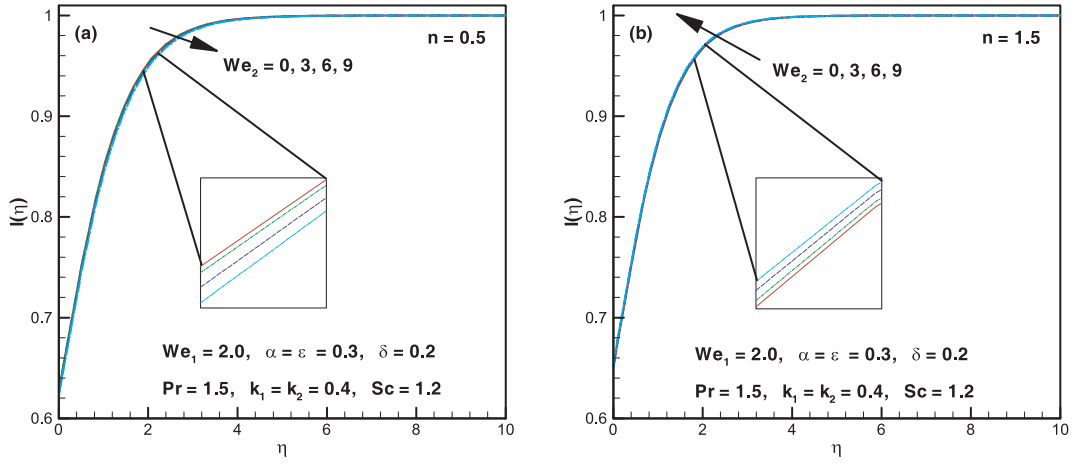

Fig. 7. (a,b): Impact of We_2 on $l(\eta)$.

concentration field $l(\eta)$ are presented in Figs. 8(a,b) and 9(a,b). The analogous trend is being recognized by uplifting the value of α and *Sc*. It is also reported the α and *Sc* are the enhancing function of Carreau liquid concentration distribution. Physically, the *Sc* is the quotient of viscous diffusion amount to the molecular diffusion amount. For that reason, advanced value of *Sc* recall the greater viscous diffusion amount, which is appropriate to strengthen the concentration of Carreau liquid revealed in Fig. 9(a,b).

Behavior of k_1 and k_2 on $l(\eta)$

To sightsee the properties of chemical reaction (homogeneous-heterogenous) parameters (k_1, k_2) for shear thinning/thickening conditions on concentration profile Figs. 10(a,b) and 11(a,b) are systematized. The concentration of a Carreau liquid in response to enlarging values of k_1 and k_2 is decay. The reactants are disbursed during the homogeneous reaction k_1 which causes the diminishing of the concentration field

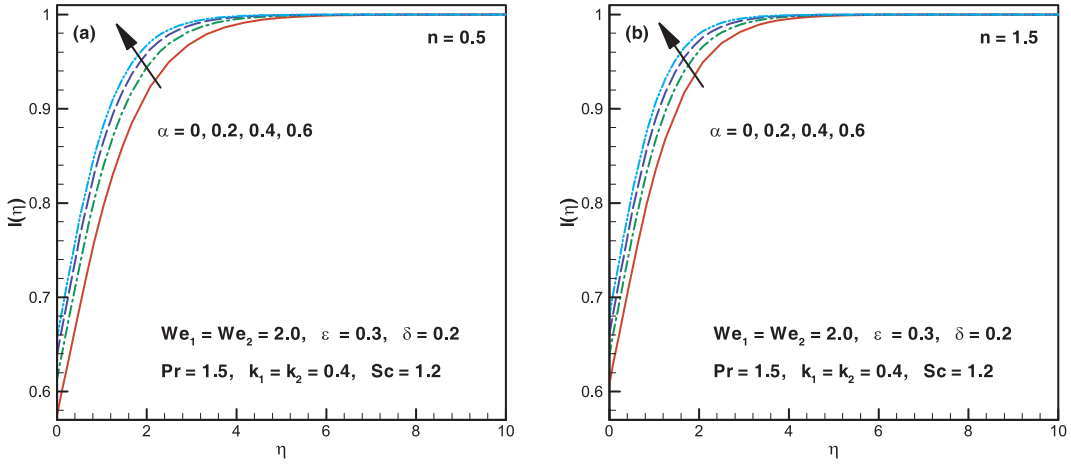

Fig. 8. (a,b): Impact of α on $l(\eta)$.

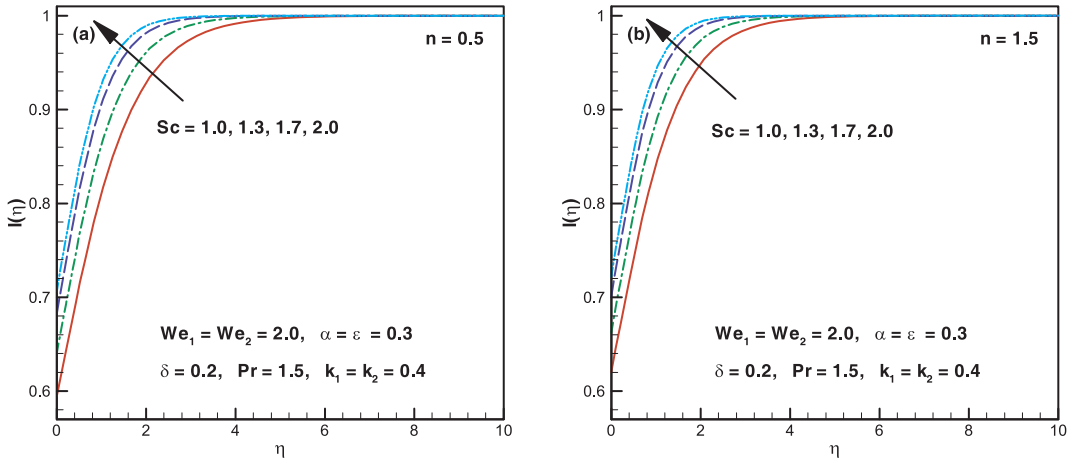

Fig. 9. (a,b): Impact of *Sc* on $l(\eta)$.

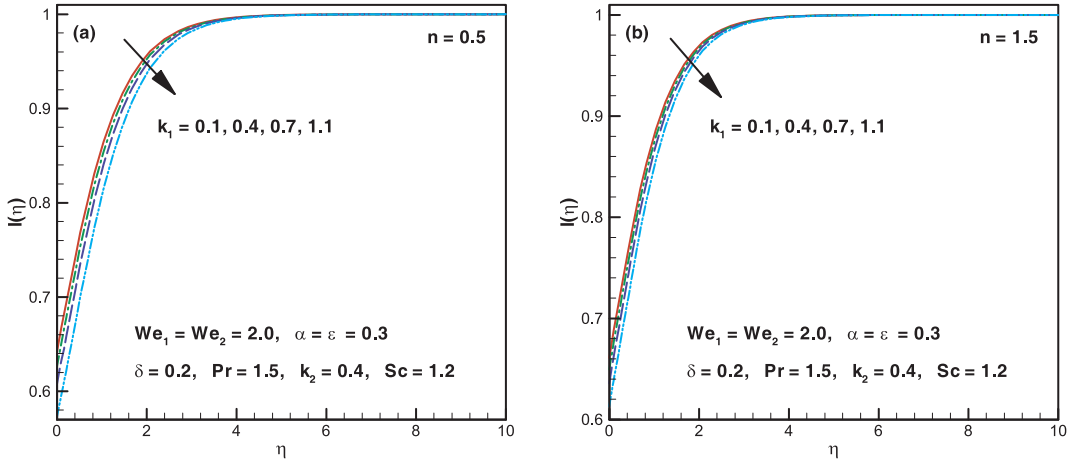

Fig. 10. (a,b): Impact of k_1 on $l(\eta)$.

which is planned in 10(a,b). Moreover, sophisticated value of heterogeneous parameter k_2 for both ($n < 1$ and $n > 1$) spectacles analogous development for concentration field. Hence, the outcomes of k_1 and k_2 are same on Carreau liquid concentration field.

Validation of numerical scheme

Graphical comparison

The graphical assessment between numerical (bvp4c) and homotopy analysis method (HAM) methods for the value of thermal relaxation and thermal conductivity parameters (β ,ϵ) respectively, are strategized in Fig. 12(a,b). These upshots spectacles a wonderful settlement between these two schemes.

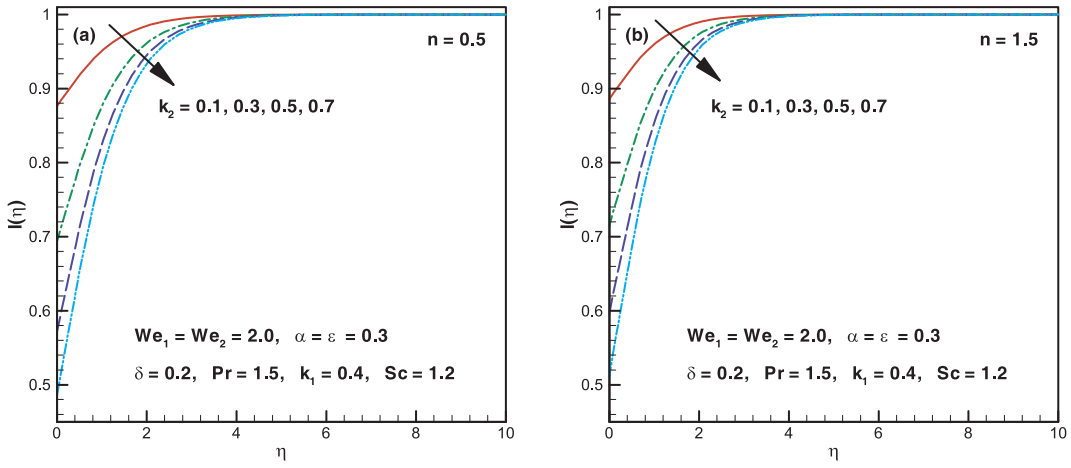

Fig. 11. (a,b): Impact of k_2 on $l(\eta)$.

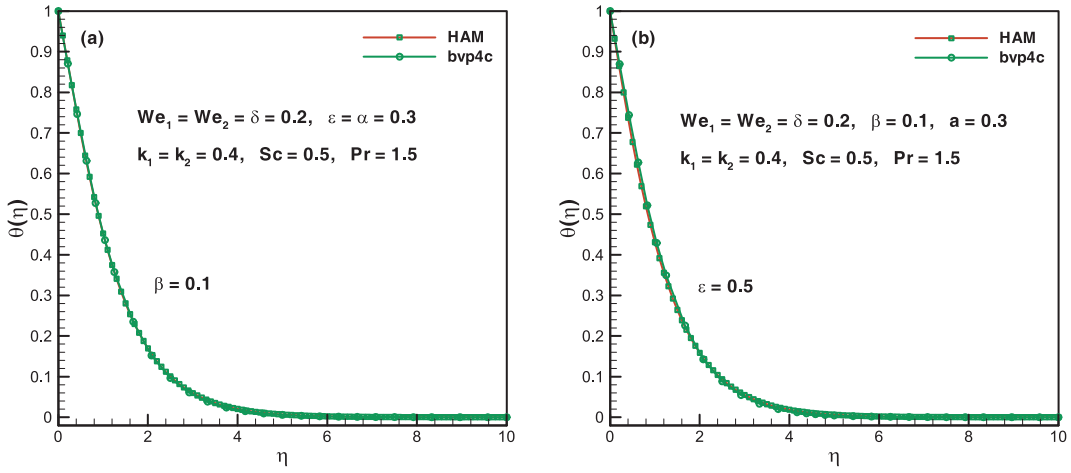

Fig. 12. (a,b): A comparison of β and ϵ on $\theta(\eta)$ for two different techniques.

Table 1
Numerical values of $f''(0)$ with two different schemes in limiting cases when $We_1 = We_2 = 0$ and $n = 3$ are fixed.

α	$f''(0)$				
	Ref. [49]	Ref. [50]	Ref. [51]	Present (bvp4c)	Present (HAM)
0.0	−1	−1	−1	−1	−1
0.25	−1.048813	−1.048813	−1.048818	−1.04880750	−1.0488067
0.50	−1.093097	−1.093096	−1.093098	−1.09309070	−1.0930905
0.75	−1.134485	−1.134486	−1.134487	−1.13448290	−1.13448275
1.0	−1.173720	−1.173721	−1.173721	−1.17372090	−1.17372091

Table 2
Numerical values of $g''(0)$ with two different schemes in limiting cases when $We_1 = We_2 = 0$ and $n = 3$ are fixed.

α	$g''(0)$				
	Ref. [49]	Ref. [50]	Ref. [51]	Present (bvp4c)	Present (HAM)
0.0	0	0	0	0	0
0.25	−0.194564	−0.194565	−0.194567	−0.19456986	−0.19456946
0.50	−0.465205	−0.465206	−0.465207	−0.46521364	−0.46521349
0.75	−0.794622	−0.794619	−0.794619	−0.79461627	−0.79461618
1.0	−1.173720	−1.173721	−1.173721	−1.17372090	−1.17372091

Tabular comparison

The legitimacy of the numerical significances is also recognized by assessment with the analytical upshots attained by the HAM as displayed in Tables 1–3. Furthermore, these outcomes are compared with earlier obtainable relevant prose as a remarkable case of the problem and brilliant settlement is noted. The table of the local Nusselt number for the different values of Prandtl number is vacant through Table 4. An assessment between numerical scheme (bvp4c) and analytical

Table 3
Numerical values of $-\theta'(0)$ with two different schemes in limiting cases when $We_1 = We_2 = \beta = \delta = \epsilon = 0$, Pr = 1 and $n = 3$ are fixed.

α	$-\theta'(0)$			
	Ref. [50]	Ref. [51]	Present (bvp4c)	Present (HAM)
0.25	0.665933	0.665939	0.66593318	0.66593302
0.50	0.735334	0.735336	0.73533293	0.73533278
0.75	0.796472	0.796472	0.79647181	0.79647179

Table 4
Numerical values of two different schemes for different values of Prandtl number when $We_1 = We_2 = \beta = \delta = \epsilon = 0$ and $n = 3$ are fixed.

Pr	$-\theta'(0)$				
	Ref. [52]	Ref. [53]	Ref. [54]	Present (bvp4c)	Present (HAM)
0.70	0.4539	0.4539	0.4539	0.45445767	0.4539331
1.0				0.58201280	0.5819772
1.3				0.69302203	0.6930220
1.6				0.79227119	0.7922980
1.8				0.85344101	0.8534274
2.0	0.9113	0.9114	0.9114	0.91134742	0.9113362
5.0				1.56806380	
7.0	1.8954	1.8954	1.8954	1.89542450	
10.0				2.30801360	
20.0	3.3539	3.3539	3.3539	3.35396200	
70.0	6.4621	6.4622	6.4622	6.46238930	

technique (HAM) with some previous prose is also presented in this table. Therefore, we are confident that the present results are very precise.

Key facts

This article explored the properties of generalized Fourier's law and chemical reaction on 3D flow of Carreau fluid subject to variable thermal conductivity and heat sink/source. The following interpretations are condensed in present analysis.

- The velocity field declined for We_1 when $(n < 1)$ and enhanced for $(n > 1)$ whereas, conflicted behavior is being established for temperature field.
- The thermal relaxation parameter β decayed the temperature field while for thermal conductivity parametre ϵ the temperature of Carreau liquid enhanced for both ($n = 0.5$ and $n = 1.5$).
- For shear thinning liquid $(n < 1)$ the impact of We_1 and We_2 were quite reversed to the shear thickening liquid on concentration field.
- Analogous trend for $(n < 1$ and $n > 1)$ of homogeneous-heterogeneous reaction parameters were detected on concentration field.

References

[1] Fourier JBJ. Theorie analytique De La Chaleur Paris; 1822.
[2] Cattaneo C. Sulla conduzione del calore. Atti Semin Mat Fis Univ Modena Reggio Emilia 1948;3:83–101.
[3] Christov CI. On frame indifferent formulation of the Maxwell-Cattaneo model of finite speed heat conduction. Mech Res Commun 2009;36:481–6.
[4] Liu L, Zheng L, Liu F, Zhang X. An improved heat conduction model with Riesz fractional Cattaneo–Christov flux. Int J Heat Mass Transf 2016;103:1191–7.
[5] Waqas M, Hayat T, Farooq M, Shehzad SA, Alsaedi A. Cattaneo-Christov heat flux model for flow of variable thermal conductivity generalized Burgers fluid. J Mol Liq 2016;220:642–8.
[6] Khan M, Ahmad L, Khan WA, Alshomrani AS, Alzahrani AK, Alghamdi MS. A 3D Sisko fluid flow with Cattaneo-Christov heat flux model and heterogeneous-homogeneous reactions: a numerical study. J Mol Liq 2017;238:16–9.
[7] Liu L, Zheng L, Liu F, Zhang X. Heat conduction with fractional Cattaneo-Christov upper-convective derivative flux model. Int J Therm Sci 2017;112:421–6.
[8] Waqas M, Khan MI, Hayat T, Alsaedi A, Khan MI. On Cattaneo-Christov double diffusion impact for temperature-dependent conductivity of Powell-Eyring liquid. Chin J Phys 2017;55:729–37.
[9] Khan WA, Irfan M, Khan M. An improved heat conduction and mass diffusion models for rotating flow of an Oldroyd-B fluid. Results Phys 2017;7:3583–9.
[10] Mustafa M, Hayat T, Alsaedi A. Rotating flow of Maxwell fluid with variable thermal conductivity: an application to non-Fourier heat flux theory. Int J Heat Mass Transf 2017;106:142–8.
[11] Ali ME, Sandeep. Cattaneo-Christov model for radiative heat transfer of magneto-hydrodynamic Casson-ferrofluid: a numerical study. Results Phys 2017;7:21–30.
[12] Dogonchi AS, Ganji DD. Impact of Cattaneo-Christov heat flux on MHD nanofluid flow and heat transfer between parallel plates considering thermal radiation effect. J Taiwan Inst Chem Eng 2017;80:52–63.
[13] Merkin JH. A model for isothermal homogeneous-heterogeneous reactions in boundary-layer flow. Math Comput Model 1996;24:125–36.
[14] Chaudhary MA, Merkin JH. A simple isothermal model for homogeneous-heterogeneous reactions in boundary-layer flow, I. Equal diffusivities. Fluid Dyn Res 1995;16:311–33.
[15] Chen J, Liu B, Gao X, Yan L, Xu D. Effects of heterogeneous–homogeneous interaction on the homogeneous ignition in hydrogen-fueled catalytic microreactors. Int J Hydrogen Energy 2016;41:11441–54.
[16] Raju CSK, Sandeep N, Saleem S. Effects of induced magnetic field and homogeneous–heterogeneous reactions on stagnation flow of a Casson fluid. Eng Sci Tech Int J 2016;19:875–87.
[17] Hayat T, Rashid M, Imtiaz M, Alsaedi A. Nanofluid flow due to rotating disk with variable thickness and homogeneous-heterogeneous reactions. Int J Heat Mass Transf 2017;113:96–105.
[18] Khan WA, Irfan M, Khan M, Alshomrani AS, Alzahrani AK, Alghamdi MS. Impact of chemical processes on magneto nanoparticle for the generalized Burgers fluid. J Mol Liq 2017;234:201–8.
[19] Gireesha BJ, Kumar PBS, Mahanthesh B, Shehzad SA, Rauf A. Nonlinear 3D flow of Casson-Carreau fluids with homogeneous–heterogeneous reactions: a comparative study. Results Phys 2017;7:2762–70.
[20] Khan MI, Waqas M, Hayat T, Khan MI, Alsaedi A. Numerical simulation of nonlinear thermal radiation and homogeneous-heterogeneous reactions in convective flow by a variable thicked surface. J Mol Liq 2017;246:259–67.
[21] Xu H. A homogeneous-heterogeneous reaction model for heat fluid flow in the stagnation region of a plane surface. Int Commun Heat Mass Transf 2017;87:112–7.
[22] Hayat T, Rashid M, Alsaedi A. Three dimensional radiative flow of magnetite-nanofluid with homogeneous-heterogeneous reactions. Results Phys 2018;8:268–75.
[23] Khan M, Irfan M, Khan WA. Thermophysical properties of unsteady 3D flow of magneto Carreau fluid in presence of chemical species: a numerical approach. J Braz Soc Mech Sci Eng 2018. http://dx.doi.org/10.1007/s40430-018-0964-4.
[24] Chamkha AJ. Hydromagnetic natural convection from an isothermal inclined surface adjacent to a thermally stratified porous medium. Int J Eng Sci 1997;35:975–86.
[25] Chamkha AJ. MHD-free convection from a vertical plate embedded in a thermally stratified porous medium with Hall effects. Appl Math Model 1997;21:603–9.
[26] Takhar HS, Chamkha AJ, Nath G. Unsteady flow and heat transfer on a semi-infinite flat plate with an aligned magnetic field. Int J Eng Sci 1999;37:1723–36.
[27] Takhar HS, Chamkha AJ, Nath G. Unsteady three-dimensional MHD-boundary-layer flow due to the impulsive motion of a stretching surface. Acta Mech 2001;146:59–71.
[28] Haq RU, Noor NFM, Khan ZH. Numerical simulation of water based magnetite nanoparticles between two parallel disks. Adv Powder Technol 2016;27:1568–75.
[29] Khan M, Irfan M, Khan WA. Impact of nonlinear thermal radiation and gyrotactic microorganisms on the Magneto-Burgers nanofluid. Int J Mech Sci 2017;130:375–82.
[30] Anwar MS, Rasheed A. A microscopic study of MHD fractional inertial flow through Forchheimer medium. Chin J Phys 2017;55:1690–703.
[31] Khan M, Irfan M, Khan WA, Ahmad L. Modeling and simulation for 3D magneto Eyring-Powell nanomaterial subject to nonlinear thermal radiation and convective heating. Results Phys 2017;7:1899–906.
[32] Hayat T, Rafique K, Muhammad T, Alsaedi A, Ayub M. Carbon nanotubes significance in Darcy-Forchheimer flow. Results Phys 2018;8:26–33.
[33] Carreau PJ. Rheological equations from molecular network theories. Trans Soc Rheol 1972;116:99–127.
[34] Sulochana C, Ashwinkumar GP, Sandeep N. Transpiration effect on stagnation-point flow of a Carreau nanofluid in the presence of thermophoresis and Brownian motion. Alex Eng J 2016;55:1151–7.
[35] Khan M, Irfan M, Khan WA, Alshomrani AS. A new modeling for 3D Carreau fluid flow considering nonlinear thermal radiation. Results Phys 2017;7:2692–704.
[36] Khan M, Irfan M, Khan WA. Numerical assessment of solar energy aspects on 3D magneto-Carreau nanofluid: a revised proposed relation. Int J Hydrogen Energy 2017;42:22054–65.
[37] Khan M, Irfan M, Khan WA. Impact of forced convective radiative heat and mass transfer mechanisms on 3D Carreau nanofluid: a numerical study. Eur Phys J Plus 2017. http://dx.doi.org/10.1140/epjp/i2017-11803-3.
[38] Irfan M, Khan M, Khan WA. Numerical analysis of unsteady 3D flow of Carreau nanofluid with variable thermal conductivity and heat source/sink. Results Phys 2017;7:3315–24.
[39] Waqas M, Khan MI, Hayat T, Alsaedi A. Numerical simulation for magneto Carreau nanofluid model with thermal radiation: a revised model. Comput Methods Appl Mech Eng 2017;324:640–53.
[40] Umavathi JC, Sheremet MA. Influence of temperature dependent conductivity of a nanofluid in a vertical rectangular duct. Int J Non-Linear Mech 2016;78:17–28.
[41] Umavathi JC, Sheremet MA, Mohiuddin S. Combined effect of variable viscosity and thermal conductivity on mixed convection flow of a viscous fluid in a vertical

channel in the presence of first order chemical reaction. Eur J Mech B Fluids 2016;58:98–108.
[42] Hayat T, Zubair M, Waqas M, Alsaedi A, Ayub M. Impact of variable thermal conductivity in doubly stratified chemically reactive flow subject to non-Fourier heat flux theory. J Mol Liq 2017;234:444–51.
[43] Al-Mudhaf A, Chamkha AJ. Similarity solutions for MHD thermosolutal Marangoni convection over a flat surface in the presence of heat generation or absorption effects. Heat Mass Transf 2005;42:112–21.
[44] Damseh RA, Al-Odat MQ, Chamkha AJ, Shannak BA. Combined effects of heat generation or absorption and first-order chemical reaction on micropolar fluid flows over a uniformly stretched permeable surface: the full analytical solution. Int J Therm Sci 2009;48:1658–63.
[45] Chamkha AJ, Alay AM. MHD free convection flow of a nanofluid past a verticle plate in the presence of heat generation or absorption effects. Chem Eng Commun 2010;198:425–41.
[46] Khan M, Hamid A. Influence of non-linear thermal radiation on 2D unsteady flow of a Williamson fluid with heat source/sink. Results Phys 2017;7:3968–75.
[47] Waqas M, Ijaz Khan M, Hayat T, Alsaedi A. Stratified flow of an Oldroyd-B nanoliquid with heat generation. Results Phys 2017;7:2489–96.
[48] Reddy PS, Chamkha AJ, Al-Mudhaf A. MHD heat and mass transfer flow of a nanofluid over an inclined vertical porous plate with radiation and heat generation/absorption. Adv Powder Technol 2017;28:1008–17.
[49] Wang CY. The three dimensional flow due to a stretching flat surface. Phys Fluids 1984;27:1915–7.
[50] Liu IC, Anderson HI. Heat transfer over a bidirectional stretching sheet with variable thermal conditions. Int J Heat Mass Transf 2008;51:4018–24.
[51] Munir A, Shahzad A, Khan M. Convective flow of Sisko fluid over a bidirectional stretching surface. PLoS One 2015;10. e0130342.
[52] Khan WA, Pop I. Boundary-layer flow of a nanofluid past a stretching sheet. Int J Heat Mass Transf 2010;53:2477–83.
[53] Wang CY. Free convection on a vertical stretching surface. J Appl Math Mech (ZAMM) 1989;69:418–20.
[54] Gorla RSR, Sidawi I. Free convection on a vertical stretching surface with suction and blowing. Appl Sci Res 1994;52:247–57.